American Mineralogist, Volume 74, pages 1337–1342, 1989

Herschelite: Morphology and growth sectors

MIZUHIKO AKIZUKI
Institute of Mineralogy, Petrology, and Economic Geology, Faculty of Science, Tohoku University, Sendai 980, Japan
HIROSTUGU NISHIDO
Hiruzen Research Institute, Okayama University of Science, Kamifukuda, Maniwa-gun, Okayama Prefecture 717-06, Japan
MASATARO FUJIMOTO
Waifu 71, Kikuti-City, Kumamoto Prefecture, 861-13, Japan

ABSTRACT

Herschelite, defined as a Na-rich zeolite with the chabazite structure, has been studied with optical and scanning electron microscopy, X-ray powder diffraction, and electron-microprobe analysis. Herschelite consists of a combination of $\{10\bar{1}0\}$, $\{0001\}$, and $\{10\bar{1}1\}$ forms, showing hexagonal symmetry $6/mmm$. The three corresponding sectors show different textures between crossed polarizers, though they are chemically homogeneous. The $(10\bar{1}0)$ face consists of fine striations normal to the *c* axis, and the corresponding sector shows fine polysynthetic twins normal to the *c* axis. The (0001) face is covered by small chabazite crystals with three rhombic $\{10\bar{1}1\}$ faces that are related by twofold rotation twins, and the {0001} sector shows a fibrous texture normal to the (0001) face. Some herschelite crystals show a biconvex lens–like form, whose surfaces consist of fine chabazite crystals with three rhombic $\{10\bar{1}1\}$ faces. Thin sections show a fibrous texture that corresponds to the fine crystals on the surface. Some herschelite crystals have a gmelinite rim whose (0001) surface consists of a spiral growth pattern. Herschelite consists of triclinic sectors with fine-scale twinning, and single herschelite crystals do not occur.

INTRODUCTION

Chabazite is a rhombohedral, Ca-rich zeolite consisting of AABBCC sequences of six-membered rings, whereas gmelinite is a hexagonal, Na-rich phase and consists of AABB sequences. Herschelite from Sicily, Italy, was described as a distinct species by Levy (1825). The crystals show a flat form parallel to the (0001) face or a biconvex lens–like form (Levy, 1825; Ulrich, 1870; von Lasaulx, 1881). Although herschelite and chabazite give essentially identical X-ray powder patterns, the minerals are chemically distinct. Mason (1962) redefined herschelite as a zeolite with the chabazite framework and Na > Ca. Nawaz and Foy (1982) suggested that herschelite was an independent mineral as well. Also, Passaglia (1970) discussed the chemical composition of chabazite. The parallel growth of chabazite and gmelinite structures is common in herschelite. Chabazite crystals are triclinic between crossed polarizers (Akizuki, 1981b) and by X-ray analysis (Smith et al., 1964; Mazzi and Galli, 1983). Phacolite, a variety of chabazite, is rich in Ca and shows complicated internal textures and triclinic symmetry between crossed polarizers (Akizuki and Konno, 1987). The crystal forms of herschelite and phacolite are, however, different.

The objective of the present study is to describe the texture of herschelites from three localities and to discuss the origin of the optical sectors and twinning using the general mechanism previously suggested by Akizuki (1986).

EXPERIMENTAL DETAILS

Herschelite crystals from three localities (Sicily, Italy; Melbourne, Australia; and Hayata, Saga Prefecture, Japan) were examined by scanning electron, phase-contrast optical, and polarized-light optical microscopes. The crystals consist of growth sectors that correspond to the crystal faces. The sectors can be observed in thin section between crossed polarizers. Also, the crystals were studied by powder and single-crystal X-ray methods. The chemical compositions of herschelite and coexisting gmelinite were determined using a Hitachi X-650 electron microprobe fitted with an EPMA 2200 energy-dispersive X-ray analyzer. H_2O was obtained by a Rigaku Thermoflex TG for powdered samples of 10–20 mg. Fe_2O_3, MgO, BaO, and SrO contents were negligibly small for all specimens, except the Sicily herschelite, for which semiquantitative analyses indicated 0.1–0.2 wt% BaO. Differences in chemical composition could not be recognized among growth sectors of each specimen. The Ca/(Ca + Na + K) ratio is 0.10–0.36, and the crystal structure is that of chabazite. Therefore, the specimens studied here are classified as herschelite.

0003–004X/89/1112–1337$02.00

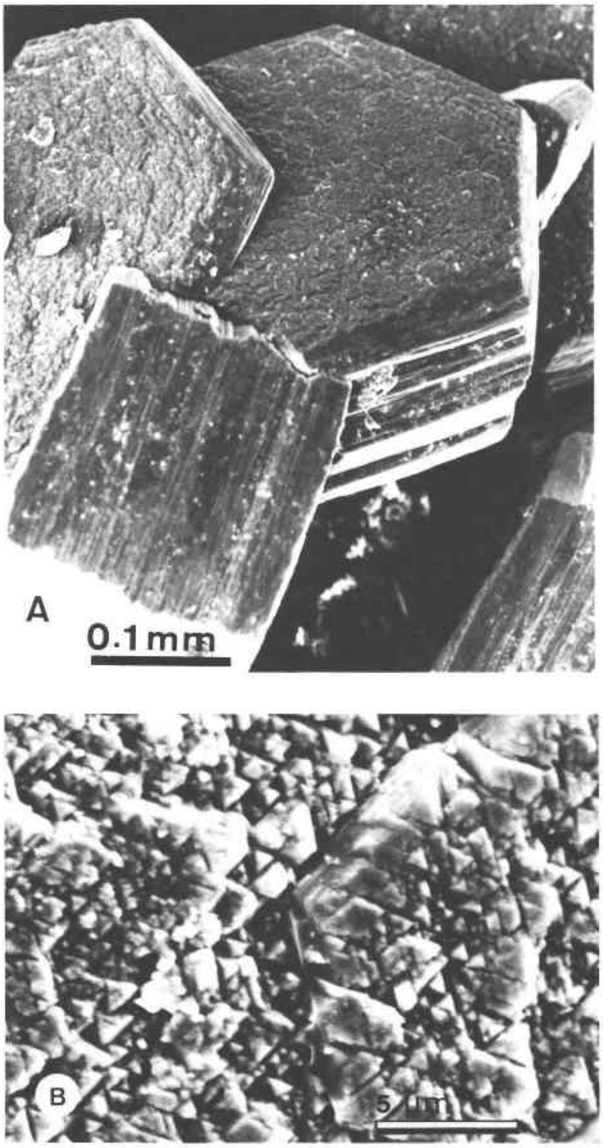

Fig. 1. (**A**) Crystal form (SEM). (**B**) A high-magnification photograph of (0001) face. The $(10\bar{1}0)$ faces exhibit striations normal to the *c* axis, and the (0001) face shows triangular crystals. Herschelite from Aci Castello, Sicily, Italy. See text for details.

DESCRIPTION OF HERSCHELITE SPECIMENS

The herschelite crystals from all three localities are Na rich and have the chabazite structure. The crystals show growth sectors with twins. The $\{0001\}$ sectors consist of fibrous crystals that are parallel or nearly parallel to the *c* axis and that are related by a rotation twin around the *c* axis. The $\{10\bar{1}0\}$ sectors, however, consist of polysynthetic twins of platy crystal parallel to (0001). The herschelite crystals are optically triclinic, although the $\{0001\}$ sector, which consists of the fibrous crystals, is uniaxial or biaxial with a small $2V$ value, because of fine twins.

Sicily specimens

The specimens from Aci Castello, Sicily, Italy, the type locality of herschelite, are about 350 μm in diameter and 200 μm in thickness. The form is hexagonal, consisting of prism faces $\{10\bar{1}0\}$ with rough striations and a basal face (0001) with a rough growth pattern (Fig. 1A). Their crystal form is slightly different from that in Gottardi and Galli (1985, p. 178). Figure 1B shows a highly magnified photograph of the (0001) face, which consists of fine triangular crystals. The fine crystals are related by a twofold axis parallel to the *c* axis, that is, by twinning. The herschelite crystals consist of $\{10\bar{1}0\}$ and $\{0001\}$ sectors between crossed polarizers. The $\{0001\}$ sector shows fine twins, which correspond to the fine triangular crystals. The $\{10\bar{1}0\}$ sector consists of fine polysynthetic twins parallel to (0001), which correspond to the striations on the $(10\bar{1}0)$ face.

Melbourne specimen

The crystal from Melbourne, Australia, is about 5 mm in diameter and 2 mm in thickness. The form is biconvex lens–like with small $(20\bar{2}1)$ and $(10\bar{1}2)$ faces and shows hexagonal $6/mmm$ symmetry. The $(20\bar{2}1)$ faces are smooth with some growth steps obvious under the optical microscope and the SEM. The $(10\bar{1}2)$ faces and convex lens–like face are covered with fine crystals with three rhombic $(10\bar{1}1)$ faces seen under the SEM at high magnification. The orientations of the fine crystals are related by a twofold axis parallel to the *c* axis.

The thin section parallel to the *c* axis was taken through the center of the crystal. The section shows a platy crystal parallel to (0001) in the center of the crystal, and the fibrous texture is elongated toward the surface with fine crystals from both sides of the plate. The platy crystal consists of a single twin of chabazite structure, and the surface of the platy crystal corresponds to the smooth $(20\bar{2}1)$ face. No prism faces were observed on the crystals. The plate shows sharp extinction, and it is suggested that the crystal is triclinic, though the area with fibrous texture exhibits wavy extinction.

Hayata specimens

In Hayata, Saga Prefecture, Japan, amygdule minerals are distributed in basalt, and of them chabazite and calcite are the most common minerals. The calcite and chabazite with rhombic faces were crystallized first, and herschelite, thomsonite, and natrolite followed (Ishibashi, 1974). Phacolite (a variety of chabazite) and gmelinite are also found in the area.

Specimen 1. The crystal is 1 to 2 mm in diameter and shows a biconvex lens–like form with $(20\bar{2}1)$ faces, which show hexagonal $6/mmm$ symmetry. X-ray analysis shows only the chabazite structure without the gmelinite structure. In the SEM, the convex lens–like faces consist of a parallel growth of fine chabazite crystals with three $(10\bar{1}1)$ faces (Fig. 2A). The $(20\bar{2}1)$ faces have some striations parallel to (0001).

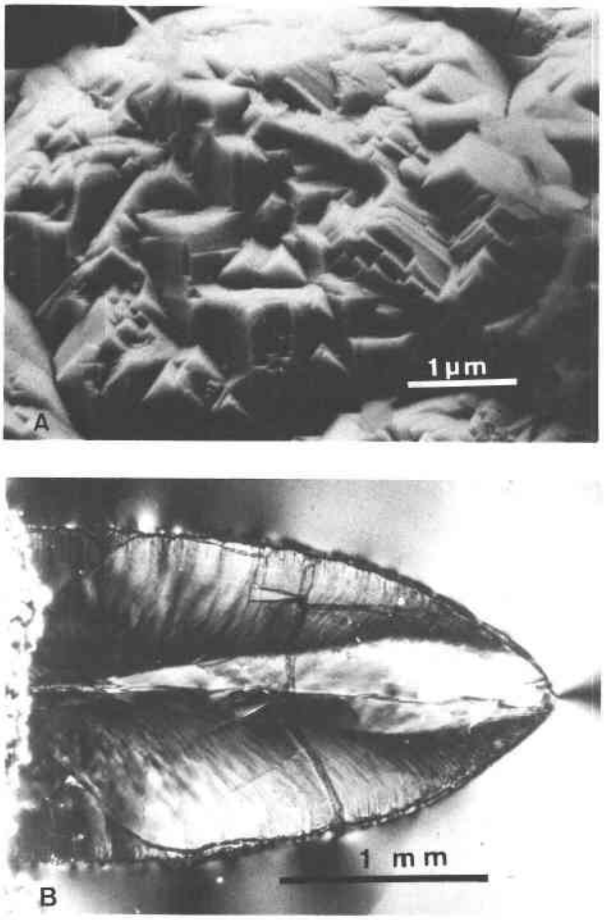

Fig. 2. Herschelite (specimen 1) from Hayata, Japan. (**A**) Fine crystals with three $(10\bar{1}1)$ faces on the convex lens–like growth surface (SEM) and (**B**) the internal texture in the thin section cut parallel to the *c* axis (between crossed polarizers).

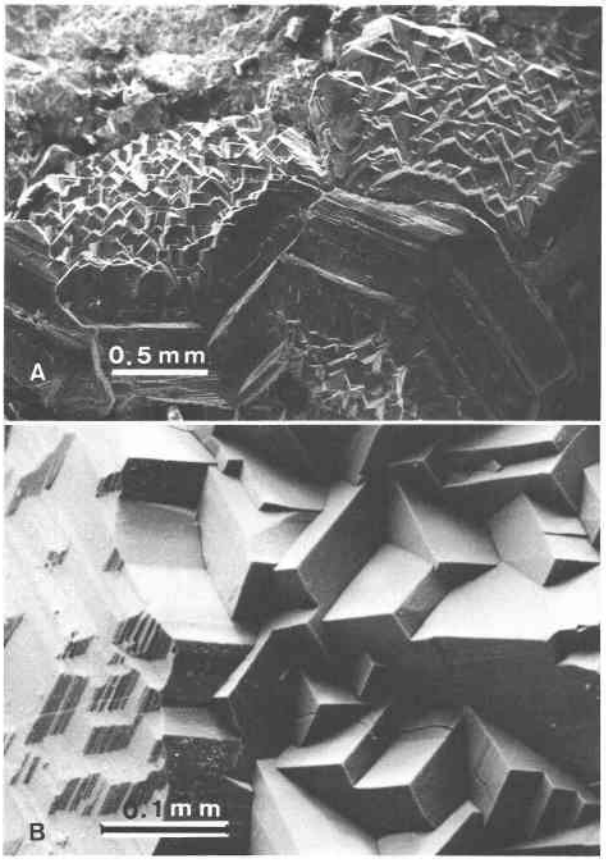

Fig. 3. Herschelite (specimen 2) from Hayata, Japan. (**A**) Low-magnification SEM photomicrograph. (**B**) High-magnification SEM photomicrograph. The crystal consists of (0001), $(10\bar{1}1)$, and $(10\bar{1}0)$ faces. The (0001) face is covered with fine crystals with rhombic $(10\bar{1}1)$ faces. Fig. 3B consists of the (0001) face with fine rhombic $(10\bar{1}1)$ faces (right), and the $(10\bar{1}1)$ face with a growth-step pattern (left). The growth patterns suggest that each $\{10\bar{1}1\}$ sector is single, whereas the {0001} sector is finely twinned.

Thin sections cut parallel to the *c* axis were taken through the center of the crystal (Fig. 2B). The core consists of a penetration twin of chabazite with rhombohedral form, from which several polysynthetic (0001) twins develop in the direction normal to the *c* axis, resulting in a platy crystal, though Figure 2B does not show the core. The platy crystal produces the $(20\bar{2}1)$ face on the crystal surface. Fine fibrous crystals are developed on both sides of the plate; they are elongated approximately normal to the convex lens–like surface. The platy crystal shows irregularly wavy extinction between crossed polarizers.

Specimen 2. Specimen 2 shows (0001), $(10\bar{1}1)$, and $(10\bar{1}0)$ faces under the SEM and consists only of chabazite. Figures 3A and 3B show (0001) and $(10\bar{1}1)$ faces that are covered by fine crystals with three $(10\bar{1}1)$ faces. Figures 4A and 4B show sketches of the crystal surface and internal texture. The $(10\bar{1}1)$ faces consist of triangular growth patterns whose orientations are alternately opposite on the six macroscopic $\{10\bar{1}1\}$ faces, that is, the six $\{10\bar{1}1\}$ sectors are related by sixling twins. The (0001) face is depressed as compared with the $\{10\bar{1}1\}$ faces, and it consists of crystals related by a twofold rotation twin parallel to the *c* axis. The $(10\bar{1}0)$ faces consist of striations parallel to the (0001) face. The thin section cut parallel to the *c* axis shows the {0001}, $\{10\bar{1}1\}$, and $\{10\bar{1}0\}$ sectors (Fig. 4B). The {0001} sector shows fine fibers nearly normal to the (0001) face, which correspond to the fine crystals on the (0001) face, and the $\{10\bar{1}0\}$ sector consists of finely polysynthetic twins parallel to (0001).

Specimen 3. The crystals are smaller than 2 mm in diameter and consist of a combination of {0001}, $\{10\bar{1}1\}$, and $\{10\bar{1}0\}$ forms, that is, the gmelinite form. The (0001) growth face shows complicated spiral patterns with low steps (Fig. 5A). The $(10\bar{1}1)$ face consists of some triangular growth hillocks with fine steps parallel to the crystal edge between two pyramidal faces. The $(10\bar{1}0)$ face consists of fine striations parallel or normal to the *c* axis.

The thin sections cut in the direction normal or parallel to the *c* axis were examined on a universal stage. The thin section parallel to the *c* axis consists of six kinds of sectors

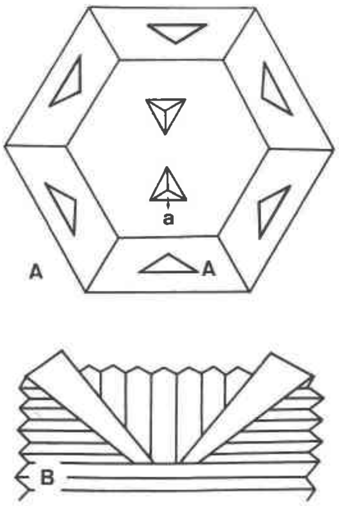

Fig. 4. Herschelite (specimen 2) from Hayata, Japan. (**A**) A schematic sketch of a growth pattern on the (0001) (center) and $(10\bar{1}1)$ (rim) faces. (**B**) A schematic sketch of the thin section in which the *c* axis is vertical. The {0001} sector consists of fibrous crystals that are related by a rotation twinning parallel to the *c* axis. The $\{10\bar{1}0\}$ sectors consist of polysynthetic twins parallel to (0001). The six $\{10\bar{1}1\}$ sectors are related by sixling twins. Each $\{10\bar{1}1\}$ sector (a and A), which is single, shows wavy extinction between crossed polarizers.

(Fig. 5B); thin rim A shows light interference colors, and the other sectors (B to F) show dark ones. X-ray analyses (precession method) show that rim A has the gmelinite structure and the other sectors (B to F) have the chabazite structure. Electron-microprobe analyses show that the rim with the gmelinite structure (analysis 6, Table 1) is richer in Na than the other sectors with the chabazite structure (analysis 5, Table 1). Rim A is thicker on the (0001) and $(10\bar{1}1)$ faces than on the $(10\bar{1}0)$ face and has more or less uniform extinction between crossed polarizers. Sectors B and C have convex lens–like interfaces and a fibrous texture that is elongated in the direction nearly normal to the interface. The interface between B and C is shown by white dashed lines in Figure 5B. The $\{10\bar{1}1\}$ sector D with fibrous texture grows on sector C. The $\{10\bar{1}0\}$ sector E consists of polysynthetic twins parallel to (0001), which produce fine striations normal to the *c* axis on the $(10\bar{1}0)$ face. Core F shows (0001) polysynthetic twin lamellae, although a penetration twin of rhombohedral chabazite crystals is observed in core F in some thin sections. The {0001} sectors B and C with a fibrous texture are optically uniaxial or biaxial with a small $2V_Z$, although the $\{10\bar{1}0\}$ sector is optically triclinic and shows various $2V$ values.

Table 1. Chemical composition and formulae on the basis of 24 oxygens of herschelites and 48 oxygens of gmelinite

	1	2	3	4	5	6
SiO_2	45.87	45.81	48.41	47.36	46.74	48.78
Al_2O_3	20.83	20.23	20.31	20.80	21.00	19.80
CaO	2.01	4.54	6.05	5.07	4.99	1.74
Na_2O	8.33	5.83	4.89	5.73	6.08	10.64
K_2O	2.10	3.16	1.71	2.26	2.57	0.19
H_2O	20.49	20.97	18.89	19.18	n.d.	n.d.
Total	99.63	100.54	100.26	100.40	81.38	81.15
B.E. (%)*	6.1	−4.9	−2.8	−1.4	−3.9	−5.1
Si	7.86	7.86	8.01	7.90	7.82	16.16
Al	4.20	4.09	3.96	4.09	4.14	7.73
Ca	0.37	0.83	1.07	0.91	0.89	0.62
Na	2.77	1.94	1.57	1.85	1.97	6.84
K	0.46	0.69	0.36	0.48	0.55	0.08
H_2O	11.70	12.00	10.43	10.67	—	—
*R***	0.10	0.24	0.36	0.28	0.26	0.08

Note: Samples are as follows: (1) Aci Castello, Sicily, Italy. (2) Melbourne, Australia. (3) Specimen 1; Hayata, Saga Prefecture, Japan. (4) Specimen 2; Hayata, Saga Prefecture, Japan. (5) Specimen 3; Hayata, Saga Prefecture, Japan. (6) Specimen 3 (gmelinite); Hayata, Saga Prefecture, Japan.

* Balance error.

** R = Ca/(Ca + Na + K).

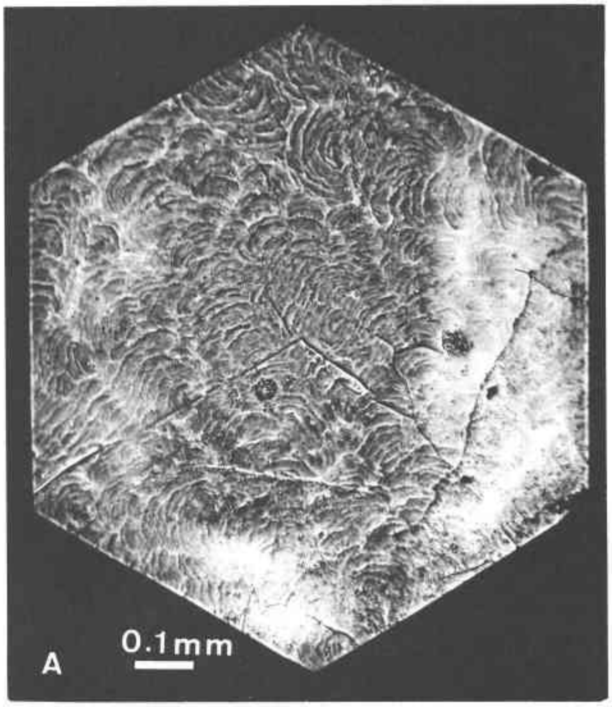

Fig. 5. Herschelite (specimen 3) from Hayata, Japan. (**A**) Spiral growth features on (0001) under a phase-contrast optical microscope. (**B**) The internal texture in the $(10\bar{1}0)$ thin section (*c* axis is vertical) between crossed polarizers. See text for details.

Discussion

Both herschelite and phacolite have a penetration-twinned core of chabazite structure, from which a singly twinned or polysynthetically twinned plate develops parallel to (0001) (Akizuki and Konno, 1987). Crystal growths, however, are different on the twinned plate between herschelite and phacolite. In herschelite, fibrous crystals with the chabazite structure develop in the direction parallel or nearly parallel to the *c* axis, resulting in a fibrous texture with a convex lens–like surface, whereas

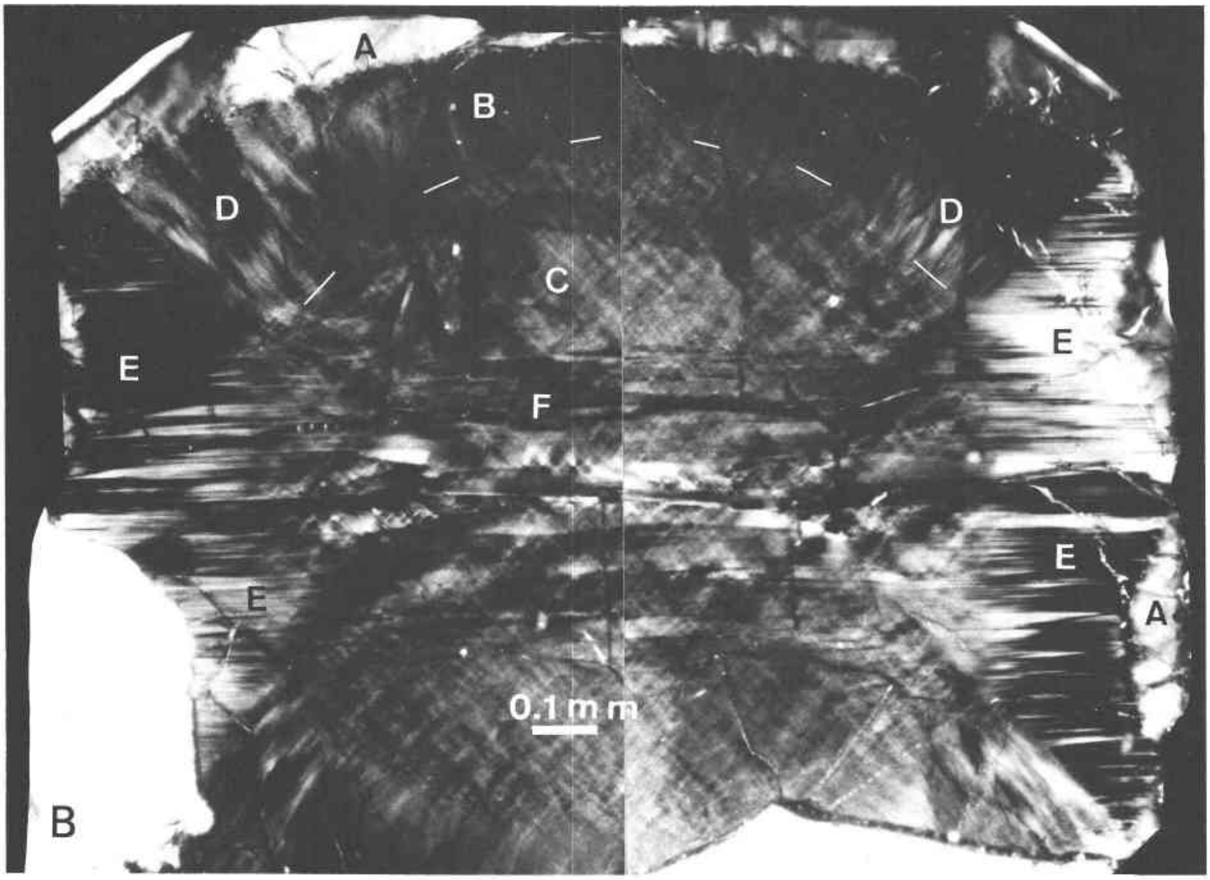

Fig. 5—*Continued.*

in phacolite, fine twin rods develop in directions normal to the *c* axis.

Chabazite with rhombohedral form is triclinic between crossed polarizers (Akizuki, 1981b) and in X-ray analysis (Mazzi and Galli, 1983). The triclinic property is attributed to the ordered arrangement of (Al^{3+},Si^{4+}) ions (Mazzi and Galli, 1983), which occurs on the surface during crystal growth (Akizuki, 1981b; Akizuki and Konno, 1987). Also, the ordered arrangement of the (Al^{3+},Si^{4+}) ions causes the herschelite structure to have triclinic symmetry. The {0001} sector consists of finely twinned crystals with the chabazite structure, and therefore the sector is optically uniaxial or biaxial with a small optic axial angle.

Chabazite consists of AABBCC sequences, and gmelinite has AABB sequences. The twinned chabazite structure (AABBCCBBAA) has the gmelinite sequence (BBCCBB) along the (0001) twin boundary. Since herschelite with a fibrous texture was produced during rapid crystal growth, the crystals could not exclude the Na ion during growth, resulting in a Na-rich zeolite with the chabazite structure. If the crystal had grown slowly under the conditions at which chabazite grows, Na ions would been excluded from the crystal, and Na-poor chabazite with the rhombohedral form would have been produced. If gmelinite sequences (AABBAA) are locally produced in herschelite during growth, the twinned chabazite structure will be produced. Because of fine-scale twinning, the prism faces developed on herschelite. If chabazite is produced in a Ca-rich solution at a high growth rate, the crystal will grow in a phacolite form. Since phacolite is rich in Ca, gmelinite sequences are not produced in the crystal during growth, and the prism faces do not develop on the crystal. Ca-rich gmelinite will be produced by the same mechanism.

The finely twinned crystals are produced on the (0001) face, resulting in the {0001} sector with a fibrous texture. Since the gmelinite rim of the Hayata specimen 3 grows on the finely twinned chabazite crystals, crystal imperfections such as a spiral dislocation are abundant in the rim, and therefore the (0001) surface has complicated spiral growth patterns.

Zeolites grow at low temperatures, and therefore the electrostatic charges of Al^{3+}, Si^{4+}, and alkali ions are balanced two dimensionally along a growth step on the surface. If a tetrahedral site forms after an alkali ion occupies the channel, an Al^{3+} ion will preferentially occupy the tetrahedral site. If, on the other hand, a tetrahedral site forms before an alkali ion occupies the channel, a Si^{4+} ion will occupy the tetrahedral site. If the growth steps are inclined to the mirror or the glide plane, the two symmetry-related sites in a crystal will not be equivalent on the surface. Thus ordering will occur, and the symmetry of the crystal will be reduced; therefore, the mirror plane changes into the twin plane. A three-dimensional crystal structure grows by a piling up of the two-dimensional structures, and therefore, the ordered arrangements of the (Al^{3+},Si^{4+}) ions are different from sector to sector, resulting in parallel-grown polycrystals showing different symmetries. The structures are frozen after the growth, because of low temperature. If the growth steps on the crystal face are circular, the (Al^{3+},Si^{4+}) order will vary along the steps, and a wavy optical extinction will be seen between crossed polarizers (i.e., Akizuki and Sunagawa, 1978; Akizuki, 1986; Akizuki and Nishido, 1988).

Similar to herschelite, stilbite is not a single phase, but consists of an orthorhombic {001} and a monoclinic twinned {110} sector (Akizuki and Konno, 1985). The orthorhombic stilbite structure grows only on the (001) face, and the monoclinic stilbite structure is produced only on the (110) face, resulting in the sectoral structure. Neither orthorhombic nor monoclinic stilbite crystals can exist independently in nature, that is, stilbite shows no single crystal form. Also, analcime that shows a so-called optical anomaly consists of cubic and tetragonal sectors that are produced on the different vicinal faces of the (211) surface (Akizuki, 1981a). Tetragonal analcime has no single crystal form. Chabazite consists of triclinic twinned sectors that occur on the vicinal faces on the $(10\bar{1}1)$ surface (Akizuki, 1981b) and thus has no triclinic single-crystal form. These zeolites consist of many sectors showing different symmetries or sectoral twins.

Herschelite has the chabazite structure and gmelinite composition, and therefore it has been thought that herschelite formed single (untwinned) crystals. Herschelite, however, consists of triclinic sectors with fine-scale twins without exception, and single herschelite crystals do not exist in nature.

ACKNOWLEDGMENT

We are sincerely grateful to David L. Bish, Los Alamos National Laboratory, for valuable suggestions and English correction of the manuscript.

REFERENCES CITED

Akizuki, M. (1981a) Origin of optical variation in analcime. American Mineralogist, 66, 403–409.

——— (1981b) Origin of optical variation in chabazite. Lithos, 14, 17–21.

——— (1986) Al-Si ordering and twinning in edingtonite. American Mineralogist, 71, 1510–1514.

Akizuki, M., and Konno, H. (1985) Order-disorder structure and the internal texture of stilbite. American Mineralogist, 70, 814–821.

——— (1987) Growth twinning in phacolite. Mineralogical Magazine, 51, 427–430.

Akizuki, M., and Nishido, H. (1988) Epistilbite: Symmetry and twinning. American Mineralogist, 73, 1434–1439.

Akizuki, M., and Sunagawa, I. (1978) Study of the sector structure in adularia by means of optical microscopy, infra-red absorption, and electron microscopy. Mineralogical Magazine, 42, 453–462.

Gottardi, Glauco, and Galli, Ermanno. (1985) Natural zeolites. Springer-Verlag, Berlin.

Ishibashi, Kiyoshi. (1974) Amygdule minerals in the Higashi-matuura basalts, Saga Prefecture, Japan. Journal of the Japanese Association of Mineralogists, Petrologists and Economic Geologists, 69, 255–266 (in Japanese with English abstract).

Levy, A. (1825) Descriptions of two new minerals. Annals of Philosophy, 10, 361–363.

Mason, Brian. (1962) Herschelite—A valid species? American Mineralogist, 47, 985–987.

Mazzi, Fiorenzo, and Galli, Ermanno. (1983) The tetragonal framework of chabazite. Neues Jahrbuch für Mineralogie, Monatschefte, 461–480.

Nawaz, Rab, and Foy, H.J. (1982) A chemical classification of the chabazite group zeolites. Irish Naturalists Journal, 20, 405–456.

Passaglia, Elio. (1970) The crystal chemistry of chabazites. American Mineralogist, 55, 1278–1301.

Smith, J.V., Knowles, C.R., and Rinaldi, F. (1964) Crystal structures with a chabazite framework: III. Hydrated Ca-chabazite at +20 and −150° C. Acta Crystallographica, 17, 374–384.

Ulrich, G.H.F. (1870) Contributions to the mineralogy of Victoria, p. 26–30. Government Printer, Melbourne, Australia.

von Lasaulx, A. (1881) Mineralogische Notizen, 1. Ueber einige ätnäische Mineralien. Zeitschrift für Kristallographie und Mineralogie, 5, 326–347.

MANUSCRIPT RECEIVED JUNE 27, 1988
MANUSCRIPT ACCEPTED JULY 17, 1989